UDC 536.46 + 620.3
DOI: 10.30838/J.PMHTM.2413.280323.61.946

INVESTIGATION OF PHOTOLUMINESCENCE OF ZnS_xSe_{1-x} AND ZnS_xSe_{1-x}: Mn NANOCRYSTALS OBTAINED BY COMBUSTION SYNTHESIS FOR OPTOELECTRIC DEVICES

PLAKHTII Ye.H.[1*], *Sen. Lect.*
VOLCHUK V.M.[2], *Dr. Sc. (Tech.), Prof.,*
SHYBKO Ok.M.[3], *PhD, Assoc. Prof.*

[1*] Department of Computer Science, Information Technology and Applied Mathematics, Prydniprovska State Academy of Civil Engineering and Architecture, 24-a, Architect Oleh Petrov St., Dnipro, 49005, Ukraine, tel. +38 (056) 745-23-72, e-mail: plakhtii.ev@gmail.com, ORCID ID: 0000-0003-3805-5026
[2] Department of Materials Science and Materials Processing, Prydniprovska State Academy of Civil Engineering and Architecture, 24-a, Architect Oleh Petrov St., Dnipro, 49005, Ukraine, tel. +38 (0562) 47-39-56, e-mail: volchuky@gmail.com, ORCID ID: 0000-0001-7199-192X
[3] Department of Computer Science, Information Technology and Applied Mathematics, Prydniprovska State Academy of Civil Engineering and Architecture, 24-a, Architect Oleh Petrov St., Dnipro, 49005, Ukraine, tel. +38 (056) 745-23-72, e-mail: ksusha2708@gmail.com, ORCID ID: 0000-0001-5894-0642

Abstract. The photoluminescence spectra of ZnS_xSe_{1-x} and ZnS_xSe_{1-x} : Mn nanocrystals obtained by combustion synthesis for all compositions with the parameter step $x = 0.2$ were registered. The movement of the maximum of the integral photoluminescence spectrum in ZnS_xSe_{1-x} and ZnS_xSe_{1-x} : Mn nanocrystals towards higher energies, depending on the parameter x, was noted. It was noticed that in the range of values $x = 0.2 \div 0.4$ there is an abrupt change in the half-width of the integral photoluminescence spectrum in ZnS_xSe_{1-x} and ZnS_xSe_{1-x} : Mn nanocrystals and the signal intensity; this may be due to the crystal lattice transformation. The parameters of the individual photoluminescence spectra of ZnS_xSe_{1-x} : Mn nanocrystals were determined by one experimental measurement based on the Tikhonov method and the derivative spectroscopy method. The nature of the individual photoluminescence bands is discussed. The difference between the integral (sum of individual bands) and experimental spectrum arises from the presence of an additional individual band of low intensity in the experimental spectrum. This individual band is located in the region of E = 2.48 eV and is associated with the electronic transitions in Mn^{2+} ions in the ZnS lattice.

Keywords: *ZnS_xSe_{1-x} nanocrystals; ZnS_xSe_{1-x} : Mn nanocrystals; combustion synthesis; photoluminescence spectra; individual emission bands*

ДОСЛІДЖЕННЯ ФОТОЛЮМІНЕСЦЕНЦІЇ НАНОКРИСТАЛІВ ZnS_xSe_{1-x} ТА ZnS_xSe_{1-x} : Mn, ОТРИМАНИХ МЕТОДОМ САМОПОШИРЮВАНОГО ВИСОКОТЕМПЕРАТУРНОГО СИНТЕЗУ ДЛЯ ОПТОЕЛЕКТРИЧНИХ ПРИЛАДІВ

ПЛАХТІЙ Є. Г.[1*], *ст. викл.,*
ВОЛЧУК В. М.[2], *докт. техн. наук, проф.,*
ШИБКО О. М.[3], *канд. техн. наук, доц.*

[1*] Кафедра комп'ютерних наук, інформаційних технологій та прикладної математики, Придніпровська державна академія будівництва та архітектури, вул. Архітектора Олега Петрова, 24-а, 49005, Дніпро, Україна, + 38 (056) 745-23-72, e-mail: plakhtii.ev@gmail.com, ORCID ID: 0000-0003-3805-5026
[2] Кафедра матеріалознавства та обробки матеріалів, Придніпровська державна академія будівництва та архітектури, вул. Архітектора Олега Петрова, 24-а, 49005, Дніпро, Україна, тел. +38 (0562) 47-39-56, e-mail: volchuky@gmail.com, ORCID ID: 0000- 0001-7199-192X
[3] Кафедра комп'ютерних наук, інформаційних технологій та прикладної математики, Придніпровська державна академія будівництва та архітектури, вул. Архітектора Олега Петрова, 24-а, 49005, Дніпро, Україна, тел. + 38 (056) 745-23-72, e-mail: ksusha2708@gmail.com, ORCID ID: 0000-0001-5894-0642

Анотація. Зареєстровано спектри фотолюмінесценції нанокристалів ZnS_xSe_{1-x} і ZnS_xSe_{1-x} : Mn, отриманих методом самопоширюваного високотемпературного синтезу, для всіх складів із кроком параметра x = 0,2. Відмічено переміщення максимуму інтегрального спектра фотолюмінесценції в нанокристалах ZnS_xSe_{1-x} і

ZnS_xSe_{1-x} : Mn у бік більш великих енергій залежно від параметра *x*. Помічено, що в діапазоні значень *x* = 0.2÷0.4 відбувається різка зміна півширини інтегрального спектра фотолюмінесценції в нанокристалах ZnS_xSe_{1-x} і ZnS_xSe_{1-x} : Mn та інтенсивності сигналу, це може бути пов'язано з перетворенням кристалічної ґратки та різкою заміною оточення іонів Mn^{2+} із сірки на селен. Використовуючи формулу для згладжування експериментального спектра фотолюмінесценії на основі методу Тихонова, отримали регуляризаційний коефіцієнт. Параметри індивідуальних спектрів фотолюмінесценції нанокристалів ZnS_xSe_{1-x} : Mn визначено за одним експериментальним вимірюванням на основі методу похідної спектроскопії. Обговорюється природа окремих смуг фотолюмінесценції. Показано, що сума шістки знайдених окремих смуг може не відповідати експериментальному спектру фотолюмінесценії. Різниця між інтегральним (сумою окремих смуг) і експериментальним спектрами виникає через наявність додаткової окремої смуги низької інтенсивності в експериментальному спектрі. Ця окрема смуга розташована в області E = 2.48 еВ і пов'язана з електронними переходами в іонах Mn^{2+} у ґратці ZnS. Отримані результати дозволяють використовувати синтезовані методом самопоширюваного високотемпературного синтезу нанокристали ZnS_xSe_{1-x} і ZnS_xSe_{1-x} : Mn для різноманітних оптоелектронних пристроїв.

Ключові слова: *нанокристали ZnS_xSe_{1-x},; нанокристали ZnS_xSe_{1-x}:Mn; самопоширюваний високотемпературний синтез; спектри фотолюмінесценції; індивідуальні смуги випромінювання*

1. Introduction

The phenomenon of photoluminescence (PL) has found wide application in various optoelectronic devices, among them: emitting LEDs, lasers, white light sources, information display devices [1−3], etc. PL analysis is an effective method of non-destructive testing; it has found application in chemistry, biology, medicine, physics, archeology, and forensics [4−6] and will be very useful in the study of new solar energy materials [7]. An analysis of the PL spectra makes it possible to obtain information about the structure of the energy levels of optically active centers in the band gap, their activation energy, the lifetime of charge carriers in an excited state, etc. Such information can be obtained by determining the parameters of the individual components of the experimental PL spectrum [8; 9]. Existing methods for determining the parameters of individual bands have their limitations. For example, the Alentsev-Fock method requires several very different spectra in which the same emission centers participate [10], λ-modulation requires the use of expensive and complex equipment [11], ORIGIN allows computer simulations that can be divorced from real physical processes [12]. Solid solutions of ZnS_xSe_{1-x} and ZnS_xSe_{1-x} : Mn nanocrystals (NCs) are promising materials for creating light-emitting diodes, lasers, luminescent matrices, white light sources, short-wave radiation photodetectors, and solar panels [13–15]. To obtain ZnS_xSe_{1-x} and ZnS_xSe_{1-x} : Mn NCs, we used the combustion synthesis method (CS), also known as self-propagating high-temperature synthesized, which is characterized by a number of advantages: short process time, the possibility of obtaining the final product in large volumes, low cost and energy consumption per unit of production, simplicity of used equipment and its environmental safety [16].

Various groups of researchers have obtained NC solid solutions ZnS_xSe_{1-x} or $ZnCd_{1-x}S_x$ by the CS method [17−22]. In this case, the individual emission bands in the photoluminescence (PL) spectra of ZnS_xSe_{1-x} : Mn NCs were partially studied by us in [21; 23], without describing the technique for obtaining and the behavior of individual bands.

2. Material and methods

Synthesis of NC of solid solutions ZnS_xSe_{1-x} and ZnS_xSe_{1-x} : Mn was carried out according to the procedure described in [20] with a parameter step x = 0,2. The characteristics of the obtained nanocrystals are presented in [17; 20].

It should be emphasized, that the crystal lattice parameters of the NC solid solutions ZnS_xSe_{1-x} and ZnS_xSe_{1-x} : Mn in the cubic phase ranged from *a* = 5.377 Å (for *x* = 1) to *a* = 5.630 Å (for x = 0). These values turned out to be smaller than the crystal lattice parameters of single crystals of ZnS_xSe_{1-x} solid solutions, which are in the range from *a* = 5.4093Å (for x = 1) to *a* = 5.6687 Å (for x = 0) [24]. This, in turn, indicates the deformation stresses

characteristic of NC. Laser diode radiation excited the PL of NC (λ_{ex} = 408 nm). The PL spectra were registered by the standard procedure at room temperature, using a photoelectronic multiplier −136 as an emission detector (Fig. 1).

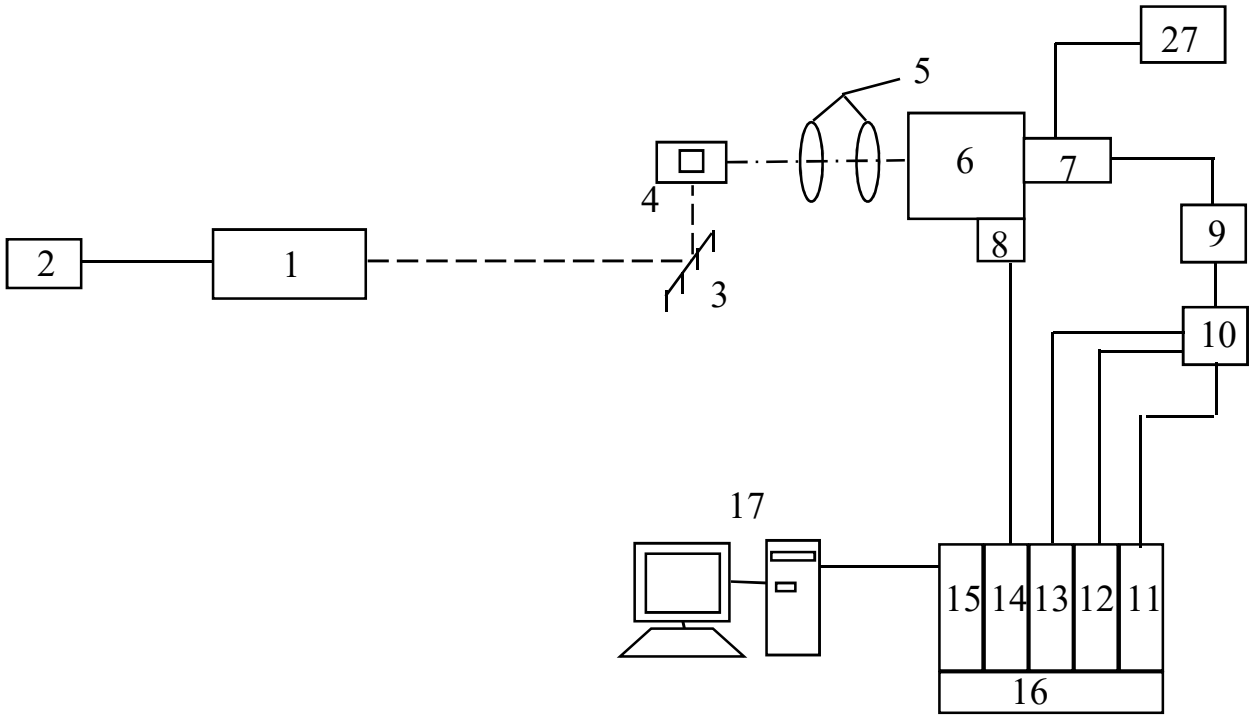

Fig. 1. Block diagram of the optical spectral complex for studying PL spectra (laser (1), power supply (2), mirror (3), quartz cryostat (4), condenser with lenses (5), entrance slit of the MDR–12 monochromator (6) , photoelectronic multiplier–136 (7), stepper motor DSHI–200–2 (8), transistor amplifier (9), two threshold discriminator (10), CAMAC system (11−16), personal computer (17))

3. Results and discussion

The PL spectra of ZnS_xSe_{1-x} NCs, which were registered at room temperature, are shown in Fig. 2, *a*. The registered maxima of the integral PL spectra of ZnS_xSe_{1-x} NCs are in the green-orange region of the spectrum, as in the works where the synthesis of ZnS_xSe_{1-x} NCs in the presence of oxygen was carried out by other methods [25; 26]. In this case, the location of the maxima of the integral PL spectra of ZnS_xSe_{1-x} NCs is quite different from the location of the maxima of the integral spectra of bulk ZnS_xSe_{1-x} crystals [27]. This case can be explained by the fact that the synthesis is carried out in an air environment and the oxidation of ZnS_xSe_{1-x} NC occurs during the reaction. It should be noted that RDA [20] did not reveal Zn_xO_y phases; however, PL is a more sensitive method [28]. It can be seen a monotonic shift of the maximum of the emission spectrum to the short-wavelength region with an increase in the parameter *x*. The PL spectra of ZnS_xSe_{1-x} NCs were characterized by a close half-width and were in the energy range of 1.6–2.4 eV. On average, the half-width of the integral PL spectrum of ZnS_xSe_{1-x} NCs is within the range of λ from 90 to 110 nm (0.43–0.48 eV) and is larger than the half-width of the bulk PL spectrum by 20–30 %, which may be due to different average sizes of NCs and microstresses inherent in synthesized NC.

It should be noted that the maximum half-width of the experimental PL spectra lies in the range of NC compositions *x* = 0,2–0,4. This can be compared with the fact that the rearrangement of the crystal lattice of ZnS_xSe_{1-x}NCs is observed in ZnS_xSe_{1-x}NCs in this range of values [20].

The registered PL spectra of ZnS_xSe_{1-x} : Mn NCs are shown in Fig. 2, *b*. The maxima of the integral PL spectra of ZnS_xSe_{1-x} : Mn NCs are in the orange region of

the spectrum and correlate with the results of other authors [28]. In this case, the location of the maxima of the integral PL spectra of ZnS_xSe_{1-x} : Mn NCs is shifted towards higher energies by 10–15 nm (E = 0.05 eV) from the maxima location of the integral spectra of bulk ZnS_xSe_{1-x} : Mn crystals. This can be explained by the fact that the main contribution to the emission of ZnS_xSe_{1-x} : Mn NCs is made by Mn^{2+} ions, the emission of which in NCs can depend on microstresses inherent in NCs. The shape of the PL spectra is asymmetric, which indicates that the integral spectra are not elementary.

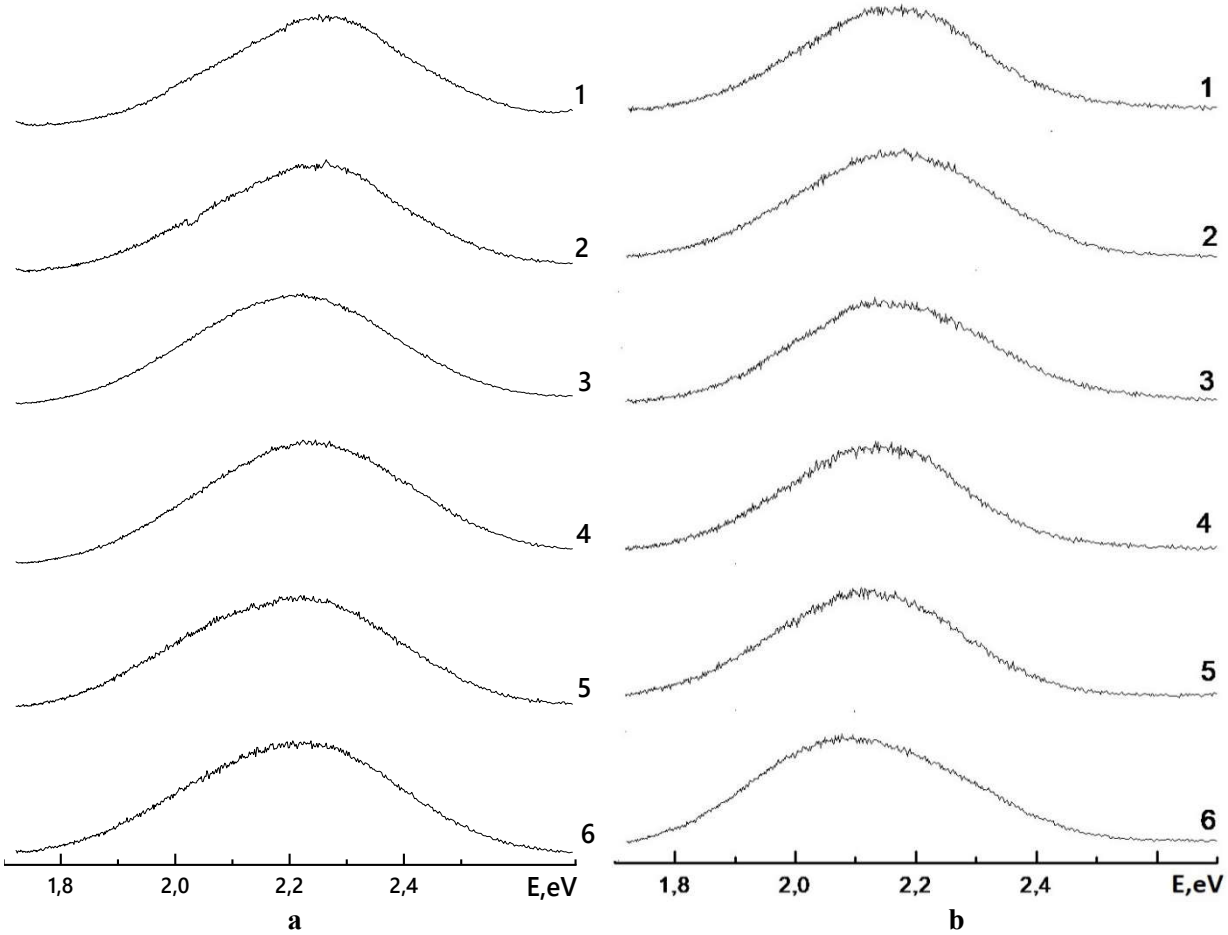

Fig. 2. PL spectra of ZnS_xSe_{1-x} (a) and ZnS_xSe_{1-x} : Mn (b) NCs depending on the parameter x: (1) – x = 1, (2) – x = 0.8, (3) – x = 0.6, (4) – x = 0.4, (5) – x = 0.2, (6) – x = 0

The half-width of the experimental PL spectra of ZnS_xSe_{1-x} : Mn NCs is in the range of 92÷114 nm (0.34–0.41 eV) and is greater than the half-width of bulk ZnS_xSe_{1-x} : Mn crystals by 10–20 nm (E = 0.05 eV). It should be noted that in the range of x = 0.2–0.4, there is a sharp decrease in the half-width of the integral PL spectrum of ZnS_xSe_{1-x} : Mn NCs and an increase in the intensity of the PL signal. This may be because Mn^{2+} ions are worse integrated into the lattice and are mainly located on the surface. The noise reaches 4–8 % at the maximum amplitude in the experimental PL spectra of ZnS_xSe_{1-x} : Mn NCs. The maximum noise amplitude was observed for $ZnS_{0.2}Se_{0.8}$: Mn and $ZnS_{0.4}Se_{0.6}$: Mn NCs, and the minimum one for ZnS : Mn NCs.

After registration of the PL spectra of ZnS_xSe_{1-x} : Mn NCs, the task was to investigate the behavior of individual PL bands depending on the composition using a single experimental measurement. We used a technique based on the derivative spectroscopy method (DSM) to solve this problem, which we applied in [29]. It consists of the following steps:

1) PL spectrum measurement;

2) determination of the nature and level of measurement noise, smoothing of the experimental PL spectrum;

3) calculation of derivatives of PL spectra and obtaining data on the number of individual bands, their intensities, maxima positions, and half-widths;

4) interpretation of the obtained results.

At the same time, it should be noted that the greater the number of experimental points registered at the first stage of the technique, the more accurate the final result obtained. Therefore, it is recommended to register spectra with the highest spectral resolution. Also, the proposed method can be applied to any spectra, such as EPR spectra, etc. [30].

In the second stage of the methodology, we smoothed the spectrum based on the Tikhonov method; therefore, the task was set:

$$\min_{f(x)} \int_X |\, g(x) - f(x)\,|^2\, dx + \alpha \int_X |\, D_1[f(x)]\,|^2\, dx, \quad (1)$$

where $D_1[f(x)] = \dfrac{df(x)}{dx}$ is an operator of differentiation and α is a regularization parameter which sets a compromise between the square error of smoothing and Euclidean norm square of the first derivative of the sought smooth function. The solution to the problem will be the ratio:

$$f = \left(\mathbf{I} + \alpha \mathbf{D}^T \mathbf{D}\right)^{-1} g, \quad (2)$$

where $\mathbf{I}$ is the identity matrix and $\mathbf{D}^T$ is the transposed matrix $\mathbf{D}$.

In this case, it is recommended to tune the operating parameters both to the current noise environment, due to the noise characteristics of the used photomultiplier, and to the maximum value of useful spectrum values, using numerical modeling. It should be emphasized that possible narrow spectral peaks must be removed before applying smoothing, as done in [31]. Using numerical modeling similar to that carried out in [32; 33], we found the regularization parameter $\alpha = 6 \cdot 10^8$.

At the third stage of the technique, according to the results of numerical modeling under the condition $\varepsilon = 0.1 \cdot I_{\max}$, where $I_{\max}$ is the maximum value of the amplitude of the PL spectrum, it was found that an acceptable estimation accuracy is achieved when using derivatives up to the sixth, seventh, and eighth orders. We used the fourth, fifth, and sixth order of the derivative for calculations. At the maximum points of the elementary components of the spectrum, the following relations must be fulfilled:

$$I(E) > \varepsilon;\ d^4I(E)/dE^4 > 0;$$

$$d^5I(E)/dE^5 = 0;\ d^6I(E)/dE^6 < 0, \quad (3)$$

where $d^4I(E)/dE^4$, $d^5I(E)/dE^5$ and $d^6I(E)/dE^6$ are the initial spectrum's fourth, fifth, and sixth derivatives. Thus, we select the "useful" area of the signal and search in this area for such E values for which all other conditions are satisfied simultaneously. The array of values that satisfy relations (3) is used to estimate the number and location of the maxima of individual bands in the PL spectrum. The ratio:

$$\sigma = 2 \cdot \sqrt{2\ln(2)} \cdot \sqrt{-5\frac{d^4I(\lambda)/d\lambda^4}{d^6I(\lambda)/d\lambda^6}}, \quad (4)$$

calculated at the points of maxima of individual bands allows estimating their half-width. Since the obtained values of the parameters of individual spectrum bands usually contain errors due to measurement noise and calculation errors, it is advisable to refine the obtained results in the future. In this paper, such refinement was performed using the least squares method with a constraint on the positivity of the residual of the solution. In addition, for its implementation, an iterative scheme of the alternating-variable descent method was used with the successive refinement of the values of the individual band parameters. Also, it is possible to obtain values of the individual band parameters based on the decomposition method of the sum of Gaussian curves, however, the use of this method is recommended for experimental spectra with "small noise", for example, registered at low temperatures [34].

The obtained results of extracting the parameters of individual bands from the integral PL spectrum are shown in Fig. 3.

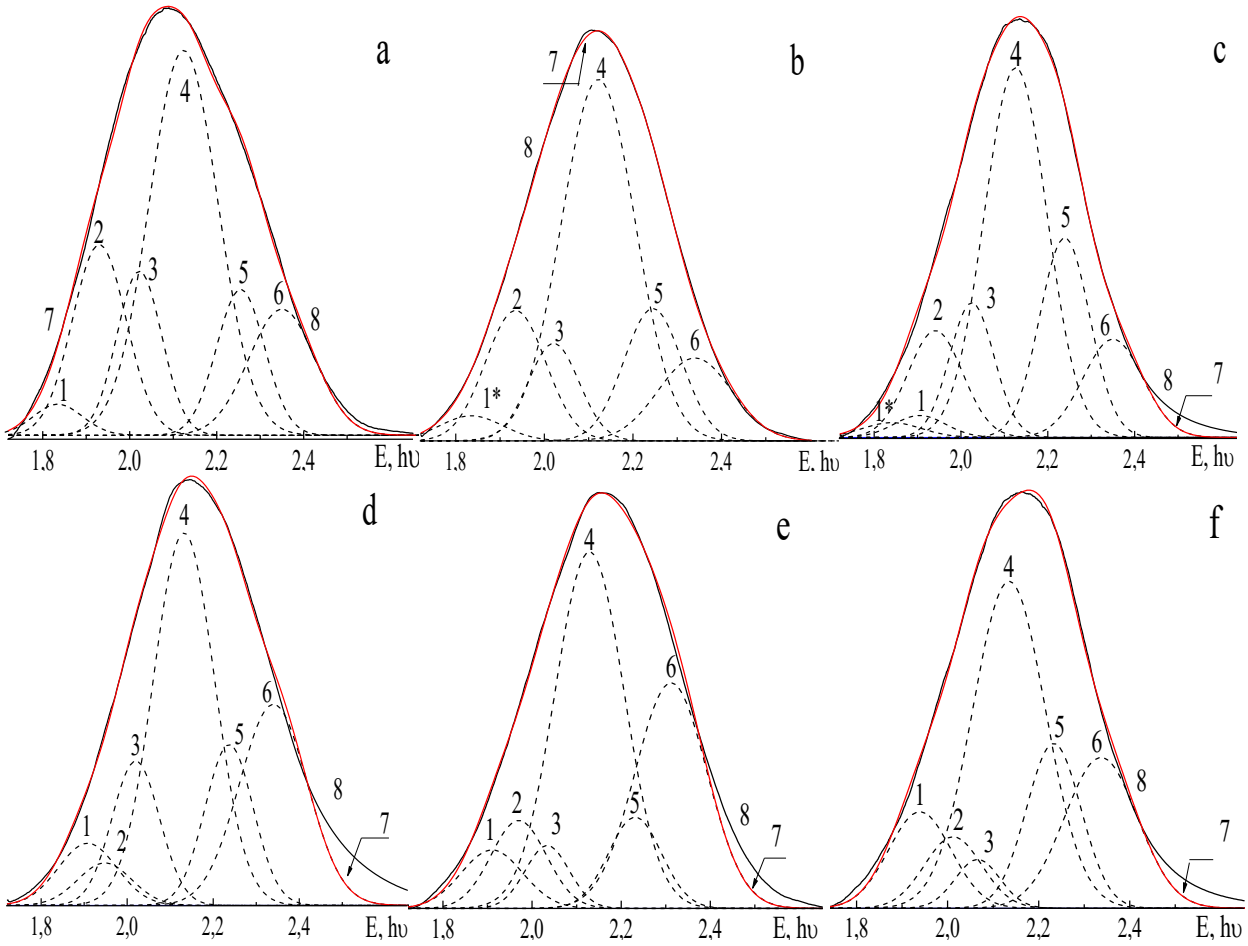

Fig. 3. PL spectra of ZnS_xSe_{1-x} :Mn NC for values of the parameter x = 0 (a), 0.2(b), 0.4(c), 0.6(d), 0.8(e), 1(f): individual PL bands with E =1.835 eV (λ_{max}= 675.5 nm) – 1, E =1.929 eV (λ_{max}= 642.5 nm) – 2, E =2.022 eV (λ_{max}= 613 nm) – 3, E =2.124 eV (λ_{max}= 583.5 nm) – 4, E =2.255 eV (λ_{max}= 550 nm) – 5, E = 2.345 eV (λ_{max}= 528.5 nm) – 6 for composition with x = 0; 7 – integral PL spectrum (sum of individual bands), 8 – experimental PL spectrum, 1 – individual PL band E=1.939 eV (λ_{max} = 639 nm) observed in compositions with x = 0.4÷1, T = 300 K*

The difference between the integral (sum of individual bands) and the experimental spectrum arises because, in the third relation, we extracted the "useful region" of the signal > 10 % of the maximum intensity of the experimental spectrum and, therefore, could miss an individual band of lower intensity. At the same time, it should be noted that this difference arises in compositions with x = 0.4–1. In these compositions, an additional individual band may appear in the region of 2.48 eV, associated, e. g. with electronic transitions in Mn^{2+} ions in the ZnS lattice, which is also observed by other authors [35].

We detected 6 individual bands with the following parameters in ZnS : Mn NCs: E = 1.939 eV (λ_{max} = 639 nm) – 1, E = 2.012 eV (λ_{max} = 616 nm) – 2, E = 2.066 eV (λ_{max} = 600 nm) – 3, E = 2.141 eV (λ_{max} = 579 nm) – 4, E= 2.233 eV (λ_{max} = 555 nm) – 5, E = 2.337 eV (λ_{max} = 530.5 nm) – 6. These emission bands are characterized by the following parameters in ZnSe : Mn NC: E = 1,835 eV (λ_{max} = 675.5 nm) – 1*, E = 1.929 eV (λ_{max} = 642.5 nm) – 2, E = 2.022 eV (λ_{max} = 613 nm) – 3, E = 2.124 eV (λ_{max} = 583.5 nm) – 4, E = 2.255 eV (λ_{max} = 550 nm) – 5, E = 2.345 eV (λ_{max} = 528.5 nm) – 6 (Fig. 4). These results correlate well with the results, we obtained earlier [20], however, there are some differences associated with different smoothing constants.

In the fourth stage of the methodology, we compare the results with the obtained ones in

other works and conclude. The results of DSM for the PL of ZnS : Mn NCs are in good agreement with the results of determining the parameters of individual bands in ZnS : Mn single crystals and in ZnS:Mn NCs [21; 29] using the Alentsev–Fock and computer simulation methods. In [21; 36; 37], the emission of individual bands 1–5 in ZnS : Mn single crystals and NCs is associated with Mn^{2+} ions located in different local environments.

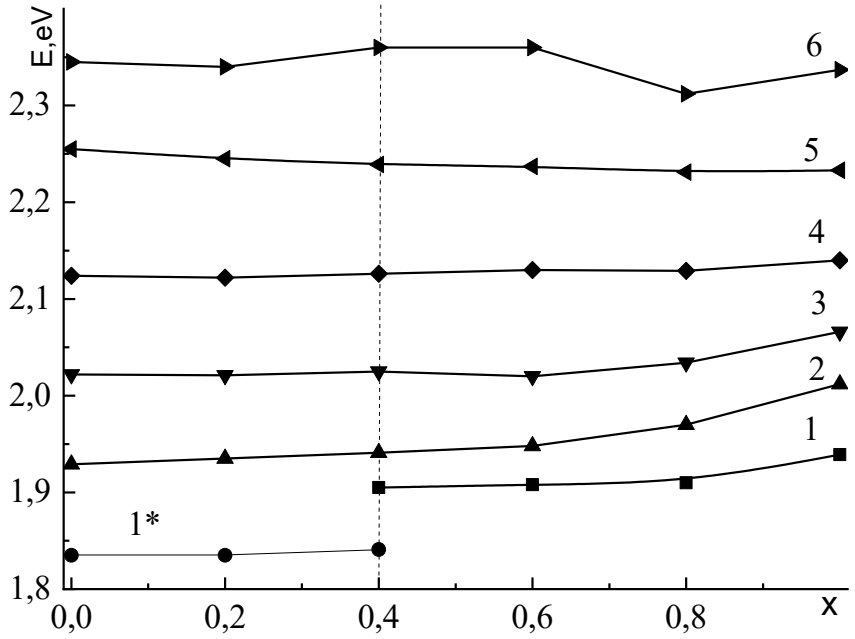

Fig. 4. Dependence of the maxima position of the elementary PL bands in ZnS_xSe_{1-x} : Mn NCs depending on the x parameter

Band 1 E = 1.939 eV (λ_{max} = 639 nm) is associated with Mn^{2+} ions in the α-MnS phase. Band 2 E = 2.012 eV (λ_{max} = 616 nm) is associated with Mn^{2+} ions surrounded by oxygen atoms or with $^4T_1$-$^6A_1$ transition of Mn^{2+} ions in the ZnS lattice. Band 3 E = 2.066 eV (λ_{max} = 600 nm) is due to Mn^{2+} ions embedded in octahedral interstices. Band 4 E = 2.135 eV (λ_{max} = 580,5 nm) is due to Mn^{2+} ions located near dislocations. Band 5 E = 2.233 eV (λ_{max} = 555 nm) is associated with Mn^{2+} ions located in the interstices of the tetrahedra of the cubic lattice, or with Mn_{Zn}. Band 6 E = 2.337 eV (λ_{max} = 530.5 nm) is associated with isolated sulfur vacancies or a copper impurity. The revealed PL bands are present in all compositions of ZnS_xSe_{1-x} : Mn.

Let us consider that the individual emission band 1* can be traced in the compositions x = 0÷0.4. In the $ZnS_{0.4}Se_{0.6}$: Mn composition, this emission band changes from E = 1.841 eV (λ_{max} = 673 nm) to E = 1.905 eV (λ_{max} = 650.5 nm) and transforms into band 1. Further, this band monotonicallythe follows the change in the width of the valence band. The behavior of individual band 1 can be related to the fact that, according to [19], ions are surrounded by selenium ions in NCs with the parameter x = 0–0.4, and Mn^{2+} ions are surrounded by sulfur ions at x = 0.4–1.

The position of the emission maximum of individual band 2 shifts towards higher energies when parameter x increases. A correlation with the width of the valence band is seen, therefore we are inclined to agree with the work [37], where this individual band is associated with the $^4T_1$ – $^6A_1$ transition of Mn^{2+} ions in ZnS_xSe_{1-x} : Mn NC.

The position of the emission maximum of individual band 3 shifts towards higher energies when parameter x increases. A correlation with the width of the valence band is seen, which occurs when the lattice parameter changes in the octahedral interstices of the ZnS_xSe_{1-x} : Mn NC.

The position of the emission maximum of the individual band 4 shifts slightly towards higher energies. It should be noted that the Mn^{2+} ions are located in dislocation regions, which are practically independent of the change

in the band gap with a change in the x parameter in the ZnS_xSe_{1-x} : Mn NC. Probably these ions are located in the region of intercrystallite layers, in which the order of particle arrangement is violated, and the concentration of impurity atoms is increased [38].

The position of the emission maximum of the individual band 5 is also unchanged. We tend to agree with those authors who associate this band with Mn_{Zn} [36].

The position of the emission maximum of the individual band 6, depending on the parameter x, is not monotonous, but abrupt and complex. Perhaps this band is not elementary. It should be also noted that the obtaining of ZnS_xSe_{1-x} : Mn NCs by the CS method is accompanied by the formation of anionic vacancies (S, Se) due to the high volatility of the anionic components.

4. Conclusion

The PL spectra of ZnS_xSe_{1-x} and ZnS_xSe_{1-x} : Mn NCs obtained by the CS method were recorded for all compositions with a parameter step x = 0.2. The movement of the maximum of the integral PL spectrum in the ZnS_xSe_{1-x} and ZnS_xSe_{1-x} : Mn NCs towards higher energies was noted, depending on the parameter x. This can be explained by an increase in the band gap of the ZnS_xSe_{1-x} NC depending on the composition x, as well as a redistribution of the intensity of the individual bands that are constituents of the PL spectrum. The operation of the PL spectrum decomposition technique based on the DSM and Tikhonov's method by a single experimental measurement is shown. A formula for smoothing the experimental PL spectrum based on the Tikhonov method is proposed. The PL spectra of ZnS_xSe_{1-x} : Mn NCs were decomposed, and the parameters of individual bands were found. It is shown that the sum of the found individual bands may not correspond to the experimental PL spectrum; the reason for this may be the individual bands are not found with an intensity of less than 10 % of the value of the integral experimental PL spectrum. The nature of the found individual bands is discussed. The obtained results realise to use of ZnS_xSe_{1-x} and ZnS_xSe_{1-x} : Mn NCs synthesized by the CS method for various optoelectronic devices.

REFERENCES

1. Adachi S. Photoluminescence properties of Mn^{4+}-activated oxide phosphors for use in white-LED applications: a review. Journal of Luminescence. 2018, vol. 202, pp. 263–281. URL: https://doi.org/10.1016/j.jlumin.2018.05.053
2. Deopa N., Rao A.S., Choudhary A., Saini S., Navhal A., Jayasimhadri M., Haranath D. and Prakash G.V. Photoluminescence investigations on Sm 3+ ions doped borate glasses for tricolor w-LEDs and lasers. Materials Research Bulletin. 2018, vol. 100, pp. 206–212. URL: https://doi.org/10.1016/j.materresbull.2017.12.019
3. Lyashkov A.Y., Makarov V.O. and Plakhtii Y.G. Structure and electrical properties of polymer composites based on tungsten oxide varistor ceramics. Ceramics International. 2022, vol. 48, no. 6, pp. 8306–8313. URL: https://doi.org/10.1016/j.ceramint.2021.12.035
4. Wang Z., Zeng H. and Sun L. Graphene quantum dots: versatile photoluminescence for energy, biomedical, and environmental applications. Journal of Materials Chemistry C. 2015, vol. 3, no. 6, pp. 1157–1165. URL: https://doi.org/10.1039/C4TC02536A
5. Skoog D.A., Holler F.J. and Crouch S.R. Principles of instrumental analysis. USA : Cengage learning, 2017, 961 p.
6. Kaszewski J., Kiełbik P., Wolska E., Witkowski B., Wachnicki Ł., Gajewski Z., Godlewski M. and Godlewski M.M. Tuning the luminescence of ZnO : Eu nanoparticles for applications in biology and medicine. Optical Materials. 2018, vol. 80, pp. 77–86. URL: https://doi.org/10.1016/j.optmat.2018.04.028
7. Lyashkov A.Y., Makarov V.O. and Plakhtii Y.G. Modeling of resettable fuses characteristics for protection of solar arrays from current overloads. Multidiscipline Modeling in Materials and Structures. 2022, vol. 18, pp. 328–338. URL: https://doi.org/10.1108/MMMS-01-2022-0010
8. Yang H., Yang S., Kong J., Dong A. and Yu S. Obtaining information about protein secondary structures in aqueous solution using Fourier transform IR spectroscopy [Text]. Nature Protocols. 2015, vol. 10, no. 3, pp. 382–396. URL: https://doi.org/10.1038/nprot.2015.024
9. Kovalenko O.V., Khmelenko O.V. and Plakhtii Y.G. Influence of heat treatment on photoluminescence spectra in ZnS : Mn crystals with hexagonal structure. Journal of Physics and Electronics. 2018, vol. 26, no. 1, pp. 73–76. URL: https://doi.org/10.15421/331812

10. Nekrasov A.A., Ivanov V.F. and Vannikov A.V. Effect of pH on the structure of absorption spectra of highly protonated polyaniline analyzed by the Alentsev–Fock method. Electrochimica Acta. 2001, vol. 46, no. 26−27, pp. 4051–4056. URL: https://doi.org/10.1016/S0013-4686(01)00693-4

11. Slyotov M.M., Gavaleshko O.S. and Kinzerska O.V. Preparation and luminescent properties of α-ZnSe heterolayers with surface nanostructure. Journal of Nano- and Electronic Physics. 2017, vol. 9, no. 5, pp. 05046. URL: https://doi.org/10.21272/jnep.9(5).05046

12. OriginPro 9.1. OriginLab Corporation, One Roundhouse Plaza, Suite 303, Northampton, MA 01060, United States. 1800-969-7720. URL: www.OriginLab.com.

13. Sadekar H.K., Ghule A.V. and Sharma R. Bandgap engineering by substitution of S by Se in nanostructured ZnS1−xSex thin films grown by soft chemical route for nontoxic optoelectronic device applications. Journal of Alloys and Compounds. 2011, vol. 509, no. 18, pp. 5525–5531. URL: https://doi.org/10.1016/j.jallcom.2011.02.089

14. Tang T.P., Wang W.L. and Wang S.F. The luminescence characteristics of ZnSxSe1− x phosphor powder. Journal of Alloys and Compounds. 2009, vol. 488, no. 1, pp. 250–253. URL: https://doi.org/10.1016/j.jallcom.2009.08.098

15. Gopi C.V., Venkata-Haritha M., Kim S.K. and Kim H.J. Improved photovoltaic performance and stability of quantum dot sensitized solar cells using Mn–ZnSe shell structure with enhanced light absorption and recombination control. Nanoscale. 2015, vol. 7, no. 29, pp. 12552–12563. URL: https://doi.org/10.1039/C5NR03291A

16. Levashov E.A., Mukasyan A.S., Rogachev A.S. and Shtansky D.V. Self-propagating high-temperature synthesis of advanced materials and coatings. International Materials Reviews. 2017, vol. 62, no. 4, pp. 203–239. URL: https://doi.org/10.1080/09506608.2016.1243291

17. Plakhtii Ye.H. *Rozrobka ta doslidzhennya novykh nanomaterialiv dlya elektroniky typu ZnSxSe1-x, stvorenykh metodom samoposhyryuvanoho vysokotemperaturnoho syntezu* [Development and research of new nanomaterials for electronics of the ZnSxSe1-x type, created by the method of self-propagating high-temperature synthesis]. *Metaloznavstvo ta termichna obrobka metaliv* [Metal Science and Heat Treatment of Metals]. 2022, vol. 4, no. 4, pp. 47–56. URL: https://doi.org/10.30838/J.PMHTM.2413.271222.47.910 (in Ukrainian).

18. Liu G., Yuan X., Li J., Chen K., Li Y. and Li L. Combustion synthesis of ZnSe with strong red emission. Materials and Design. 2016, vol. 97, pp. 33–44. URL: https://doi.org/10.1016/j.matdes.2016.02.063

19. Tian Z., Chen Z., Yuan X., Cui W., Zhang J., Sun S. and Liu G. Preparation of ZnSe powder by vapor reaction during combustion synthesis. Ceramics International. 2019, vol. 45, no. 14, pp. 18135–18139. URL: https://doi.org/10.1016/j.ceramint.2019.05.321

20. Kovalenko A.V., Plakhtii Y.G. and Khmelenko O.V. The peculiarities of the properties of ZnS_xSe_{1-x} nanocrystals obtained by self-propagating high-temperature synthesis. Functional Materials. 2018, vol. 4, pp. 665. URL: https://doi.org/10.15407/fm25.04.665

21. Kovalenko A.V., Plakhtii Y.G. and Khmelenko O.V. Research of Photoluminescence Spectra of ZnS_XSe_{1-X} : Mn Nanocrystals Obtained by Method of Self-propagation High-temperature Synthesis. Journal of Nano- and Electronic Physics. 2019, vol. 11, no. 4, pp. 04031-1−04031-5. URL: https://doi.org/10.21272/jnep.11(4).04031

22. Kovalenko A.V., Plakhtii Y.G. and Khmelenko O.V. Crystal Structure of ZnxCd1-xS Nanocrystals Obtained by Self-Propagating High-Temperature Synthesis. Journal of Nano- and Electronic Physics. 2022, vol. 14, no. 1, pp. 01017 (5 pp). URL: https://doi.org/10.21272/jnep.14(1).01017

23. Plakhtii Y.G. and Khmelenko O.V. Crystal structure and photoluminescence of ZnSe and ZnSe : Mn nanocrystals obtained by combustion synthesis. Physica Scripta. 2023, vol. 98, no. 3, pp. 035804. URL: https://doi.org/10.1088/1402-4896/acb5ca

24. Taguchi T., Kawakami Y. and Yamada Y. Interface properties and the effect of strain of ZnSe/ZnS strained-layer superlattices. Physica B: Condensed Matter. 1993, vol. 191, no. 1−2, pp. 23–44. URL: https://doi.org/10.1016/0921-4526(93)90176-7

25. Alghamdi Y. Composition and band Gap controlled AACVD of ZnSe and ZnS_xSe_{1-x} thin films using novel single Source precursors. Materials Sciences and Applications. 2017, vol. 8, no. 10, pp. 726–737. URL: https://doi.org/10.4236/msa.2017.810052

26. Wang Z., Zhan X., Wang Y., Safdar M., Niu M., Zhang J., Huang Y. and He J. ZnO/ZnS_xSe_{1-x} core/shell nanowire arrays as photoelectrodes with efficient visible light absorption. Applied Physics Letters. 2012, vol. 101, no. 7, pp. 073105. URL: https://doi.org/10.1063/1.4745918

27. Trubaieva O.G., Chaika M.A. and Zelenskaya O.V. Mixed ZnS_xSe_{1-x} crystals as a possible material for alpha-particle and X-ray detectors. Ukrainian Journal of Physics. 2018, vol. 63, no. 6, pp. 546–551. URL: https://doi.org/10.15407/ujpe63.6.546

28. Voitovich A.P., Kalinov V.S., Martynovich E.F., Novikov A.N. and Stupak A.P. Luminescent method for determining low concentrations of a substance in optically dense media. Journal of Applied Spectroscopy. 2011, vol. 78, no. 5, pp. 725–732. URL: https://doi.org/10.1007/s10812-011-9524-8

29. Kovalenko A.V., Plakhtiy E.G. and Vovk S.M. Application of derivative spectroscopy method to photoluminescence in ZnS : Mn nanocrystals. Ukrainian Journal of Physical Optics. 2018, vol. 19, no. 3, pp. 133–138. URL: https://doi.org/10.3116/16091833/19/3/133/2018

30. Kovalenko O.V., Plakhtii Y.G., Khmelenko O.V. and Vorovsky V.Y. The analysis of the EPR spectra in ZnO : Mn nanocrystals using the derivative spectroscopy method. Journal of Physics and Electronics. 2019, vol. 27, no. 2, pp. 89–92. URL: https://doi.org/10.15421/331931

31. Kovalenko A.V., Vovk S.M. and Plakhtii Y.G. Removal of Narrow Spectral Lines from Experimental Photoluminescence Spectra of ZnS : Mn Nanocrystals. Journal of Applied Spectroscopy. 2020, vol. 87, no. 6, pp. 995–999. URL: https://doi.org/10.1007/s10812-021-01099-2.

32. Kovalenko O.V., Vovk S.M. and Plakhtii Y.G. Method of smoothing photoluminescence spectra. Journal of Physics and Electronics. 2018, vol. 26, no. 2, pp. 73–80. URL: https://doi.org/10.15421/331828

33. Kovalenko O.V., Vovk S.M. and Plakhtii Y.G. Smoothing photoluminescence spectra and their derivatives for identification of individual bands. Functional Materials. 2020, vol. 27, no. 2, pp. 424–233. URL: https://doi.org/10.15407/fm27.02.424

34. Kovalenko A.V., Vovk S.M. and Plakhtii Y.G. Sum Decomposition Method for Gaussian Functions Comprising an Experimental Photoluminescence Spectrum. Journal of Applied Spectroscopy. 2021, vol. 88, no. 2, pp. 357–362. URL: https://doi.org/10.1007/s10812-021-01182-8.

35. Yang R.D., Tripathy S., Tay F.E., Gan L.M. and Chua S.J. Photoluminescence and micro-Raman scattering in Mn-doped ZnSnanocrystalline semiconductors. Journal of Vacuum Science & Technology B: Microelectronics and Nanometer Structures Processing, Measurement and Phenomena. 2003, vol. 21, no. 3, pp. 984–988. URL: https://doi.org/10.1116/1.1568350

36. Bacherikov Y.Y., Gilchuk A.V., Zhuk A.G., Kurichka R.V., Okhrimenko O.B., Zelensky S.E. and Kravchenko S.A. Nonmonotonic behavior of luminescence characteristics of fine-dispersed self-propagating high-temperature synthesized ZnS : Mn depending on size of its particles. Journal of Luminescence. 2018, vol. 194, pp. 8–14. URL: https://doi.org/10.1016/j.jlumin.2017.09.010

37. Li X., Zhang F., Ma C., Deng Y., Zhang L., Lu Z. and He N. Controlling the morphology of ZnS : Mn2+ nanostructure in hydrothermal process using different solvents and surfactants. Nanoscience and Nanotechnology Letters. 2013, vol. 5, no. 2, pp. 271–276. URL: https://doi.org/10.1166/nnl.2013.1495

38. Ghica D., Stefan M., Ghica C. and Stan G.E. Evaluation of the Segregation of Paramagnetic Impurities at Grain Boundaries in Nanostructured ZnO Films. ACS Applied Materials & Interfaces. 2014, vol. 6, no. 16, pp. 14231–14238. URL: https://doi.org/10.1021/am5035329

СПИСОК ВИКОРИСТАНИХ ДЖЕРЕЛ

1. Adachi S. Photoluminescence properties of Mn^{4+}-activated oxide phosphors for use in white-LED applications: a review. *Journal of Luminescence*. 2018. Vol. 202. Pp. 263–281. URL: https://doi.org/10.1016/j.jlumin.2018.05.053

2. Deopa N., Rao A. S., Choudhary A., Saini S., Navhal A., Jayasimhadri M., Haranath D., Prakash G. V. Photoluminescence investigations on Sm 3+ ions doped borate glasses for tricolor w-LEDs and lasers. *Materials Research Bulletin*. 2018. Vol. 100. Pp. 206–212. URL: https://doi.org/10.1016/j.materresbull.2017.12.019

3. Lyashkov A. Y., Makarov V. O., Plakhtii Y. G. Structure and electrical properties of polymer composites based on tungsten oxide varistor ceramics. *Ceramics International*. 2022. Vol. 48, № 6. Pp. 8306–8313. URL: https://doi.org/10.1016/j.ceramint.2021.12.035

4. Wang Z., Zeng H., Sun L. Graphene quantum dots : versatile photoluminescence for energy, biomedical, and environmental applications. *Journal of Materials Chemistry C*. 2015. Vol. 3, № 6. Pp. 1157–1165. URL: https://doi.org/10.1039/C4TC02536A

5. Skoog D. A., Holler F. J., Crouch S. R. Principles of instrumental analysis. USA : Cengage learning, 2017. 961 p.

6. Kaszewski J., Kiełbik P., Wolska E., Witkowski B., Wachnicki Ł., Gajewski Z., Godlewski M., Godlewski M. M. Tuning the luminescence of ZnO : Eu nanoparticles for applications in biology and medicine. *Optical Materials*. 2018. Vol. 80. Pp. 77–86. URL: https://doi.org/10.1016/j.optmat.2018.04.028

7. Lyashkov A. Y., Makarov V. O., Plakhtii Y. G. Modeling of resettable fuses characteristics for protection of solar arrays from current overloads. *Multidiscipline Modeling in Materials and Structures*. 2022. Vol. 18. Pp. 328–338. URL: https://doi.org/10.1108/MMMS-01-2022-0010

8. Yang H. Yang S., Kong J., Dong A., Yu S. Obtaining information about protein secondary structures in aqueous solution using Fourier transform IR spectroscopy [Text]. *Nature Protocols*. 2015. Vol. 10, № 3. Pp. 382–396. URL: https://doi.org/10.1038/nprot.2015.024

9. Kovalenko O. V., Khmelenko O. V., Plakhtii Y. G. Influence of heat treatment on photoluminescence spectra in ZnS : Mn crystals with hexagonal structure. *Journal of Physics and Electronics*. 2018. Vol. 26, № 1. Pp. 73–76. URL: https://doi.org/10.15421/331812

10. Nekrasov A. A., Ivanov V. F., Vannikov A. V. Effect of pH on the structure of absorption spectra of highly protonated polyaniline analyzed by the Alentsev–Fock method. *Electrochimica Acta*. 2001. Vol. 46, № 26-27. Pp. 4051–4056. URL: https://doi.org/10.1016/S0013-4686(01)00693-4

11. Slyotov M. M., Gavaleshko O. S., Kinzerska O. V. Preparation and luminescent properties of α-ZnSe heterolayers with surface nanostructure. *Journal of Nano-and Electronic Physics*. 2017. Vol. 9, № 5. Pp. 05046. URL: https://doi.org/10.21272/jnep.9(5).05046

12. OriginPro 9.1. OriginLab Corporation, One Roundhouse Plaza, Suite 303, Northampton, MA 01060, United States. 1800-969-7720. URL: www.OriginLab.com

13. Sadekar H. K., Ghule A. V., Sharma R. Bandgap engineering by substitution of S by Se in nanostructured ZnS1−xSex thin films grown by soft chemical route for nontoxic optoelectronic device applications. *Journal of Alloys and Compounds*. 2011. Vol. 509, № 18. Pp. 5525–5531. URL: https://doi.org/10.1016/j.jallcom.2011.02.089

14. Tang T. P., Wang W. L., Wang S. F. The luminescence characteristics of ZnSxSe1− x phosphor powder. *Journal of Alloys and Compounds*. 2009. Vol. 488, № 1. Pp. 250–253. URL: https://doi.org/10.1016/j.jallcom.2009.08.098

15. Gopi C. V., Venkata-Haritha M., Kim S. K., Kim H. J. Improved photovoltaic performance and stability of quantum dot sensitized solar cells using Mn–ZnSe shell structure with enhanced light absorption and recombination control. *Nanoscale*. 2015. Vol. 7, № 29. Pp. 12552–12563. URL: https://doi.org/10.1039/C5NR03291A

16. Levashov E. A., Mukasyan A. S., Rogachev A. S., Shtansky D. V. Self-propagating high-temperature synthesis of advanced materials and coatings. *International Materials Reviews*. 2017. Vol. 62, № 4. Pp. 203–239. URL: https://doi.org/10.1080/09506608.2016.1243291

17. Плахтій Є. Г. Розробка та дослідження нових наноматеріалів для електроніки типу ZnSxSe1-x, створених методом самопоширюваного високотемпературного синтезу. *Металознавство та термічна обробка металів*. 2022. № 4. С. 47–56. URL: https://doi.org/10.30838/J.PMHTM.2413.271222.47.910

18. Liu G., Yuan X., Li J., Chen K., Li Y., Li L. Combustion synthesis of ZnSe with strong red emission. *Materials & Design*. 2016. Vol. 97. Pp. 33–44. URL: https://doi.org/10.1016/j.matdes.2016.02.063

19. Tian Z., Chen Z., Yuan X., Cui W., Zhang J., Sun S., Liu G. Preparation of ZnSe powder by vapor reaction during combustion synthesis. *Ceramics International*. 2019. Vol. 45, № 14. Pp. 18135–18139. URL: https://doi.org/10.1016/j.ceramint.2019.05.321

20. Kovalenko A. V., Plakhtii Y. G., Khmelenko O. V. The peculiarities of the properties of ZnS_xSe_{1-x} nanocrystals obtained by self-propagating high-temperature synthesis. *Functional Materials*. 2018. Vol. 4. Pp. 665. URL: https://doi.org/10.15407/fm25.04.665

21. Kovalenko A. V., Plakhtii Y. G., Khmelenko O. V. Research of Photoluminescence Spectra of ZnS_XSe_{1-X} : Mn Nanocrystals Obtained by Method of Self-propagation High-temperature Synthesis. *Journal of Nano- and Electronic Physics*. 2019. Vol. 11, № 4. Pp. 04031-1−04031-5. URL: https://doi.org/10.21272/jnep.11(4).04031

22. Kovalenko A. V., Plakhtii Y. G., Khmelenko O. V. Crystal Structure of ZnxCd1-xS Nanocrystals Obtained by Self-Propagating High-Temperature Synthesis. *Journal of Nano- and Electronic Physics*. 2022. Vol. 14, № 1. Pp. 01017 (5 pp). URL: https://doi.org/10.21272/jnep.14(1).01017

23. Plakhtii Y. G., Khmelenko O. V. Crystal structure and photoluminescence of ZnSe and ZnSe : Mn nanocrystals obtained by combustion synthesis. *Physica Scripta*. 2023. Vol. 98, № 3. Pp. 035804. URL: https://doi.org/10.1088/1402-4896/acb5ca

24. Taguchi T., Kawakami Y., Yamada Y. Interface properties and the effect of strain of ZnSe/ZnS strained-layer superlattices. *Physica B : Condensed Matter*. 1993. Vol. 191, № 1−2. Pp. 23–44. URL: https://doi.org/10.1016/0921-4526(93)90176-7

25. Alghamdi Y. Composition and band Gap controlled AACVD of ZnSe and ZnS_xSe_{1-x} thin films using novel single source precursors. *Materials Sciences and Applications*. 2017. Vol. 8, № 10. Pp. 726–737. URL: https://doi.org/10.4236/msa.2017.810052

26. Wang Z., Zhan X., Wang Y., Safdar M., Niu M., Zhang J., Huang Y., He J. ZnO/ZnS_xSe_{1-x} core/shell nanowire arrays as photoelectrodes with efficient visible light absorption. *Applied Physics Letters*. 2012. Vol. 101, № 7. Pp. 073105. URL: https://doi.org/10.1063/1.4745918

27. Trubaieva O. G., Chaika M. A., Zelenskaya O. V. Mixed ZnS_xSe_{1-x} crystals as a possible material for alpha-particle and X-ray detectors. *Ukrainian Journal of Physics*. 2018. Vol. 63, № 6. Pp. 546–551. URL: https://doi.org/10.15407/ujpe63.6.546

28. Voitovich A. P., Kalinov V. S., Martynovich E. F., Novikov A. N., Stupak A. P. Luminescent method for determining low concentrations of a substance in optically dense media. *Journal of Applied Spectroscopy*. 2011. Vol. 78, № 5. Pp. 725–732. URL: https://doi.org/10.1007/s10812-011-9524-8

29. Kovalenko A. V., Plakhtiy E. G., Vovk S. M. Application of derivative spectroscopy method to photoluminescence in ZnS : Mn nanocrystals. *Ukrainian Journal of Physical Optics*. 2018. Vol. 19, № 3. Pp. 133–138. URL: https://doi.org/10.3116/16091833/19/3/133/2018

30. Kovalenko O. V., Plakhtii Y. G., Khmelenko O. V., Vorovsky V. Y. The analysis of the EPR spectra in ZnO : Mn nanocrystals using the derivative spectroscopy method. *Journal of Physics and Electronics*. 2019. Vol. 27, № 2. Pp. 89–92. URL: https://doi.org/10.15421/331931

31. Коваленко А. В., Вовк С. М., Плахтий Е. Г. Метод удаления узких спектральных линий из экспериментальных спектров фотолюминесценции на основе нанокристаллов ZnS : Mn. *Журнал прикладной спектроскопии*. 2020. Т. 87, № 6. С. 861–866.

32. Kovalenko O. V., Vovk S. M., Plakhtii Y. G. Method of smoothing photoluminescence spectra. *Journal of Physics and Electronics*. 2018. Vol. 26, № 2. Pp. 73–80. URL: https://doi.org/10.15421/331828

33. Kovalenko O. V., Vovk S. M., Plakhtii Y. G. Smoothing photoluminescence spectra and their derivatives for identification of individual bands. *Functional Materials*. 2020. Vol. 27, № 2. Pp. 424–233. URL: https://doi.org/10.15407/fm27.02.424

34. Коваленко А. В., Вовк С. М., Плахтий Е. Г. Метод декомпозиции суммы гауссовых функций, составляющих экспериментальный спектр фотолюминесценции. *Журнал прикладной спектроскопии*. 2021. Т. 88, № 2. С. 297–302.

35. Yang R. D., Tripathy S., Tay F. E., Gan L. M., Chua S. J. Photoluminescence and micro-Raman scattering in Mn-doped ZnS nanocrystalline semiconductors. *Journal of Vacuum Science & Technology B : Microelectronics and Nanometer Structures Processing, Measurement and Phenomena*. 2003. Vol. 21, № 3. Pp. 984–988. URL: https://doi.org/10.1116/1.1568350

36. Bacherikov Y. Y., Gilchuk A. V., Zhuk A. G., Kurichka R. V., Okhrimenko O. B., Zelensky S. E., Kravchenko S. A. Nonmonotonic behavior of luminescence characteristics of fine-dispersed self-propagating high-temperature synthesized ZnS : Mn depending on size of its particles. *Journal of Luminescence*. 2018. Vol. 194. Pp. 8–14. URL: https://doi.org/10.1016/j.jlumin.2017.09.010

37. Li X., Zhang F., Ma C., Deng Y., Zhang L., Lu Z., He N. Controlling the morphology of ZnS : Mn2+ nanostructure in hydrothermal process using different solvents and surfactants. *Nanoscience and Nanotechnology Letters*. 2013. Vol. 5, № 2. Pp. 271–276. URL: https://doi.org/10.1166/nnl.2013.1495

38. Ghica D., Stefan M., Ghica C., Stan G. E. Evaluation of the Segregation of Paramagnetic Impurities at Grain Boundaries in Nanostructured ZnO Films. *ACS Applied Materials & Interfaces*. 2014. Vol. 6, № 16. Pp. 14231–14238. URL: https://doi.org/10.1021/am5035329

Надійшла до редакції: 12.02.2023.